Performance of an Alpha-type Stirling Refrigerator with shell and tube condenser and evaporator

Eldesouki I. Eid[a], *Wael M. EL-Maghlany*[c], *Reda A. Khalaf-Allah*[a], *Ahmed M. Soliman*[b], *Salwa M. Mohamed*[a]

a Mechanical Department, Faculty of Industrial Education, Suez University, Suez, Egypt
b Engineering Science Department, Faculty of Petroleum and Mining Engineering, Suez University, Suez, Egypt
c Mechanical Engineering Department, Faculty of Engineering, Alexandria University, Alexandria, Egypt

Keywords:
alpha Stirling refrigerator, coefficient of performance, shell and tube, cooling load.

Abstract:

This paper investigates the performance of an alpha type Stirling refrigerator using shell and tube heat exchanger as evaporator and condenser with helium as a working fluid. The refrigerator is an alpha configuration. The pistons synchronization is driven by a crank-shift mechanism. A computer program in a form of spreadsheet was prepared to solve the refrigerator cycle numerically in the vision of Schmidt theory. The studied parameters are; dimensions of evaporator, condenser, and regenerator, stroke/bore ratio, speed, and phase angle. The study is directed towards the determination of the parameters that result in higher cooling load with a considerable coefficient of performance. The results show that, the refrigerator develops 0.00096 TR/cc, COP/COP $_{Carnot}$ = 0.1346 at 750 rpm. The comparison among the present work and previous ones shows that; the present refrigerator explores an enhancement in COP up to 100%, especially at low-speed levels.

Nomenclature

Symbols	**Description, unit**
A	Surface area, m^2
a	Cross-section area, m^2
D	Cylinder bore, m
d	Diameter, m
f	Friction factor
h	Heat transfer coefficient, w/m^2k
i	wire mesh, *pores/inch*
k	Thermal conductivity, w/mk
L	Length, m
m	Mass, kg
$\dot{m}$	Mass flow rate, kg/s
N	Speed, *rpm*
NTU	Number of transfer units
P	Pressure, pa
$\dot{Q}$	Heat transfer rate, W
R	Specific gas constant, $J/kg\,K$
r	Crank radius, m
Re	Reynolds number
St	Stanton number
Pr	Prandtl number
T	Temperature, K
t	Time, sec
U	Overall heat transfer coefficient, w/m^2k
V	Volume, m^3
v	Velocity m/s

Greek Letters:

α	Phase angle, rad
ε	Regenerator effectiveness,
θ	Crank angle, rad
$\beta 2$, $\beta 1$	Connecting rod angle rad
μ	Viscosity, $kg\ m/s$
ρ	Density, kg/m^3
ψ	Porosity

Subscripts:

ch	Charging
cl	Clearance
$cond$	Condenser
ev	Evaporator
hyd	Hydraulic
max	Maximum
i	Inner conditions
o	Outer conditions
P	Piston
r	Regenerator
Sh	Schmidt
T	Tube
TP	Transport Port
t	Total
w	wire of regenerator
cw	Cooling water
C	Compression space
E	Expansion space

1. Introduction

THE Stirling cycle equipment has various using in many fields as generators, engines, power devices, and cooling machines or heat pumps. In these applications, Stirling cycle has the benefits of permitting the use of different sources of energy and avoiding environmentally dangerous refrigerants. During the 1990s there was global concern about various environmental issues because of using the organic compounds such as Chlorofluorocarbons (CFC) and Hydro chlorofluorocarbons (HCFC) as refrigerants in refrigeration and air-conditioning equipment such as a household refrigerator, [1]. This has led to deplete the ozone layer and has aroused the world's attention so Many countries have tried to study and face this problem. As well as rising fuel and energy prices, prompting researchers to work on innovative energy conversion technologies, developing new technology based on high-efficiency thermal dynamics cycles and working on alternative cooling methods such as the sterling refrigerator, which can use safe and natural refrigerant fluids such as helium, nitrogen and hydrogen so The Stirling refrigeration cycle has no effect on depletion of the ozone layer, [2]. Also efficiency is high, size is small, weight is light, and power consumption is low, work without noise and very low vibrations. Recently the Stirling cooling cycle is using widely as a cooler for high-temperature superconducting devices and infrared sensors and applied to the household and commercial refrigerators due to its environmentally friendly, [3]. Alpha, beta, and Gamma Configurations are three mains types for Stirling machines. In the alpha type a displacer is not used. Have two power pistons in discrete cylinders mounted at each side of the condenser, regenerator and evaporator. In the beta type; the piston and the displacer incorporated into the same cylinder. the gamma types have two different cylinders one for the piston and the other for the displacer, The piston cylinder connected to the displacer cylinder by using links, The displacer transfers the working gas among the compression and expansion spaces through the evaporator, the regenerator, and the condenser, [4]. Although they are have a different mechanical design, they have the alike thermodynamic process, [5].

The selection of alpha-type refrigerator is referred to it are the simplest to understand, and are the easiest to construct than beta and gamma configuration. It's also easy to minimize the dead volume in the compression and expansion spaces; there is no opportunity for the occurrence of any early mixing of the hot and cold working fluid, [6]. The investigation of the refrigerators depends primarily on Schmidt theory, [7,8] the assumption of Schmidt theory are; no pressure loss in the heat exchangers and no inner pressure differences, the expansion process and the compression process changes isothermally, working gas conditions changed as an ideal gas, there is perfect regeneration, the dead expansion space maintained at expansion gas temperature, the dead compression space maintained at the compression gas temperature during the cycle, the regenerator temperature maintained at an average temperature of the compression and expansion temperature, expansion and compression spaces change according to a sine curve. The present study assenting to the suitable dimensions of the condenser, evaporator, and wire mesh regenerator as dimensionless ratios of the cylinder diameter. Stirling cycle was designed and tested the alpha type integral Stirling Refrigerator, Pistons are driven by a crank-shift mechanism and are V-shaped, under various rotating speeds and charged pressures were investigated the power consumption and the COP. The results showed that the cooling capacity increased with the charged pressure up to 1.0 MPa in case of nitrogen and up to 1.3 MPa in case of helium. Helium was better than nitrogen; The COP had a highest value about 600 rpm optimum rotational speed for nitrogen, and for helium around 900 rpm, [9]. Alpha Stirling cycle refrigerator was using air as a working gas. The charge pressure of the Stirling cycle refrigerator was taken between 2 and 5 bar, Angular speed 1000 rpm. There was found that the coefficient of performance (COP) of the Stirling cycle refrigerator was decreased at the charge pressure more than 2 bar studied by [10]. Experimental prototype was a hybrid refrigerator that combined effect of the active magnetic refrigeration with effect of the Stirling gas regenerative refrigeration. With helium working gas and charged pressure is 1 MPa the results of this study showed that the cooling performance is improved by 24% for the hybrid effects compared with using only the Stirling gas refrigeration effect studied by [11]. The design and experimental testing of a Stirling cooler that had used air as the working fluid, the results of several tests conducted under different operating conditions shown that the effect of refrigerating is very strong and allows good performance, [12]. The effect of many parameters such as dead volume ratio, working fluids, the ratio of the compression volume to the expansion volume, and the phase difference between power piston and displacer was studied on Beta type Stirling cycle machine of 100 W capacities which Designed and tested. From their results, they found that the refrigeration by using helium was 28% more than refrigeration by using nitrogen, [13]. Thermodynamic analysis of the V-type Stirling-cycle Refrigerator was, and the Refrigerator performance was investigated for three different working fluids; the hydrogen, helium and air. At the engine speed 1000 rpm, Phase angle 90^o and Charge pressure 150 kPa. The results were showed when the hydrogen was used as the working fluid; the Refrigerator COP was higher than the Refrigerator that used air or helium, [14].

The alpha Stirling refrigerator employing helium had been modeled and simulated numerically. The mathematical model was investigated serves as a comprehensive representation of the operation of a Stirling fridge. The results showed a clear temperature difference between the two chambers, a net cooling power of 1.9705 J per cycle, and a COP of 1.2616 by [15]. A hybrid refrigerator combining magnetic refrigeration effect and the effect of Stirling cycle refrigeration at chamber temperature was designed and tested. Helium gas was used as the working fluid. Under a pressure of 5.5 MPa, realistic phase angle of 60° was determined for optimizing the hybrid refrigerator cooling performance. Powers of Cooling 40.3 W and 56.4 W were achieved over temperature ranged of 15 K and 12 K, respective on. By increasing up to 28.5% in the hybrid mode when compared with the cooling power generated by the pure Stirling cycle, [16]. Parametric study of a Beta Strling prototype under different operating and geometrical parameters were performed. The model showed a good concordance with the experimental results. Results showed the optimal speed to the maximum COP was different from to the maximum cooling capacity. To achieve maximum refrigeration power, regenerator porosity must be about 85%, [17].

An integrated refrigerator combined of Stirling cycle refrigerator and Stirling cycle engine used for cooling. The duplex Stirling refrigerator was investigated thermodynamically by considering the different parameters as the compression ratios for heat engine and refrigerator, and the temperature ratios for both sides. And its effect on the overall coefficient of performance of the duplex Stirling refrigerator studied by [18]. Studying the optimizing of COP and net refrigeration of Stirling cryocooler operate at a hot end temperature of 300 K and 80 K as a cold end temperature. By optimizing multi mesh regenerator to be COP and net refrigeration considerably higher than using a single mesh regenerator by [19].

CFD model computational fluid dynamic software was used to study of the various parameters on the cooling capability of a small-scale alpha type Stirling Cryocooler. With Charge pressure 2 bar, working fluid is nitrogen the parametric study confirmed that a phase angle of 90° was required for best performance, but also showed that a regenerator porosity of 50% would be desirable. The study also showed that increasing the lengths of the heat exchangers would improve performance up to a certain length 142mm developed by [20].

In the present work, the performance of alpha type Stirling refrigerator with shell and tube condenser and evaporator is studied. The selection of this type of heat exchanger referred to the ease of manufacture, long life time, quite cheap, compactness, reliability, and suitable for the alpha refrigerator. This study is concerned with the appropriate dimensions of the evaporators, condenser, and regenerator as dimensionless ratios of the cylinder diameter. The pistons stroke, the charging pressure, and the refrigerator speed shown for the selected heat exchangers.

2. Alpha Refrigerator

The alpha Stirling Refrigerator consists of a compression space and an expansion space filled with helium as a working fluid and a wire mesh regenerator as shown in figure (1). The refrigerator has a warm heat exchanger (condenser) to exchange heat between the working fluid and the high temperature sink. It has also a cold heat exchanger (evaporator) to absorb heat from a low temperature source. The space is compressed or expanded by two pistons have a phase angle of α. The cylinder has a bore of 0.1 m.

The reciprocation of the pistons controlled via drive mechanism shown in Fig. 2. Rods join the crankshaft at a radius r and an angle θ from the expansion cylinder axis, [21].

The variation of both expansion and compression is expressed as follows:

International Journal of Scientific & Engineering Research Volume 10, Issue 2, February-2019
ISSN 2229-5518

$$X_{p1} = L_p + L\cos(\beta_1) + r\cos\theta \quad (1)$$

$$X_{p2} = L_p + L\cos(\beta_2) + r\sin\theta \quad (2)$$

$$\beta_1 = \cos^{-1}(r/L\sin\theta) \quad (3)$$

$$\beta 2 = \cos^{-1}(r/L\cos\theta) \quad (4)$$

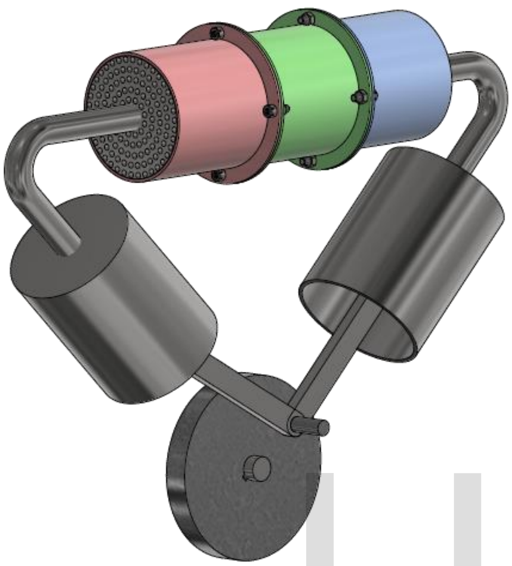

Figure (1) Scheme of the workspaces of the proposed alpha type Stirling Refrigerator.

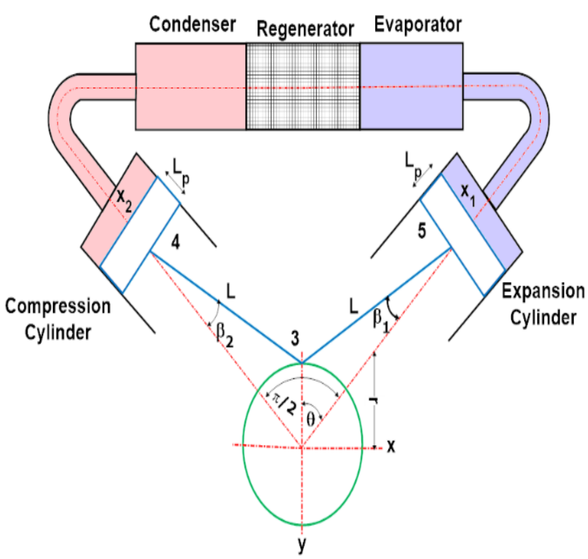

Figure (2) Dimensions mechanism.

The X-movements of both pistons are represented in Fig. 3, where, one can get pistons strokes and phase angle between them

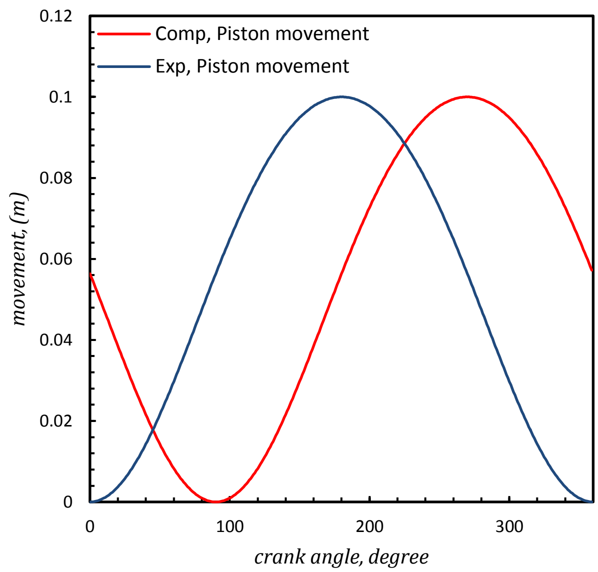

Figure (3) Piston movement versus crank angle.

The variation of both expansion and compression expressed as follows

$$V_C(\theta) = \frac{\pi}{4} DC^2 * (X_{p1(max)} - X_{p1(\theta)}) \quad (5)$$

$$V_E(\theta) = \frac{\pi}{4} DE^2 * (X_{p2(max)} - X_{p2(\theta)}) \quad (6)$$

The total volume of the refrigerator workspace expressed as follows:

$$V_{cl,C} = \frac{\pi}{4} DC^2 * L_{cl,C} \quad (7)$$

$$V_{cl,E} = \frac{\pi}{4} DE^2 * L_{cl,E} \quad (8)$$

$$V_{ev} = \frac{\pi}{4} d_{T,i}^2 * L_{T,ev} * n_{T,ev} \quad (9)$$

$$V_{cond} = \frac{\pi}{4} d_{T,i}^2 * L_{T,cond} * n_{T,cond} \quad (10)$$

$$V_r = \frac{\pi}{4} d_r^2 * L_r * \Psi \quad (11)$$

$$V_{TP,C} = \frac{\pi}{4} d_{TP,C}^2 * L_{TP,C} \quad (12)$$

$$V_{TP,E} = \frac{\pi}{4} d_{TP,E}^2 * L_{TP,E} \quad (13)$$

$$V_t = V_C(\theta) + V_E(\theta) + V_{cl,C} + V_{cl,E} + V_{ev} + V_{cond} + V_r + V_{TP,C} + V_{TP,E} \quad (14)$$

The in-between temperature of the regenerator T_r is:

$$T_r = \frac{T_C - T_E}{\ln \frac{T_C}{T_E}} \quad (15)$$

The mass of the fluid is:

$$m_{ch} = \frac{P_{ch} * V_{t,max}}{R * T_{ch}} \quad (16)$$

The momentarily Schmidt pressure is:

$$P_{Sh} = \frac{m_t * R}{\frac{V_C(\theta)+V_{cl,C}+V_{cond}+V_{TP.C}}{T_C}+\frac{V_r}{T_r}+\frac{V_E(\theta)+V_{cl,E}+V_{ev}+V_{TP,E}}{T_E}} \quad (17)$$

Referring to Fig. 4; and applying the mass conservation equation among the spaces of the refrigerator [22]

$$m_E = \frac{P_{Sh} * V_E}{R * T_E} \quad (18)$$

$$m_{ev} = \frac{P_{Sh} * V_{ev}}{R * T_E} \quad (19)$$

$$m_{cl,E} = \frac{P_{Sh} * V_{cl,E}}{R * T_E} \quad (20)$$

$$m_{TP,E} = \frac{P_{Sh} * V_{TP,E}}{R * T_E} \quad (21)$$

$$m_C = \frac{P_{Sh} * V_C}{R * T_C} \quad (22)$$

$$m_{cond} = \frac{P_{Sh} * V_{cond}}{R * T_c} \quad (23)$$

$$m_{cl,C} = \frac{P_{Sh} * V_{cl,C}}{R * T_C} \quad (24)$$

$$m_{TP,C} = \frac{P_{Sh} * V_{TP,C}}{R * T_C} \quad (25)$$

$$m_r = \frac{P_{Sh} * V_r}{R * T_r} \quad (26)$$

$$m_t = m_E + m_{ev} + m_{cl,E} + m_{TP,E} + m_C + m_{cond} + m_{cl,C} + m_{TP,C} + m_r \quad (27)$$

$$\Delta(m_E + m_{cl,E})_{\theta=n} = (m_E + m_{cl,E})_{\theta=n+1} - (m_E + m_{cl,E})_{\theta=n} \quad (28)$$

$$\Delta(m_{TP,E})_{\theta=n} = (m_{TP,E})_{\theta=n+1} - (m_{TP,E})_{\theta=n} \quad (29)$$

$$\Delta(m_{ev})_{\theta=n} = (m_{ev})_{\theta=n+1} - (m_{ev})_{\theta=n} \quad (30)$$

$$\Delta(m_r)_{\theta=n} = (m_r)_{\theta=n+1} - (m_r)_{\theta=n} \quad (31)$$

$$\Delta(m_{cond})_{\theta=n} = (m_{cond})_{\theta=n+1} - (m_{cond})_{\theta=n} \quad (32)$$

$$\Delta(m_{TP,C})_{\theta=n} = (m_{TP,C})_{\theta=n+1} - (m_{TP,C})_{\theta=n} \quad (33)$$

$$\Delta(m_C + m_{cl,C})_{\theta=n} = (m_C + m_{cl,C})_{\theta=n+1} - (m_C + m_{cl,C})_{\theta=n} \quad (34)$$

$$\frac{\Delta(m_{TP,E})_{\theta=n}}{\Delta T} = (\dot{m}_{E\to TP,E})_{\theta=n} - \left(\dot{m}_{TP,E\to ev}\right)_{\theta=n} \quad (35)$$

$$\frac{\Delta(m_{ev})_{\theta=n}}{\Delta T} = \left(\dot{m}_{TP.E\to ev}\right)_{\theta=n} - \left(\dot{m}_{ev\to r}\right)_{\theta=n} \quad (36)$$

$$\frac{\Delta(m_r)_{\theta=n}}{\Delta T} = (\dot{m}_{ev\to r})_{\theta=n} - (\dot{m}_{r\to cond})_{\theta=n} \quad (37)$$

$$\frac{\Delta(m_{cond})_{\theta=n}}{\Delta T} = (\dot{m}_{r\to cond})_{\theta=n} - (\dot{m}_{cond\to TP,C})_{\theta=n} \quad (38)$$

$$\frac{\Delta(m_{TP,C})_{\theta=n}}{\Delta T} = (\dot{m}_{cond\to TP,C})_{\theta=n} - (\dot{m}_{TP,C\to C})_{\theta=n} \quad (39)$$

$$\frac{\Delta(m_C)_{\theta=n}}{\Delta T} = \left(\dot{m}_{TP,C\to C}\right)_{\theta=n} - 0 \quad (40)$$

$$(\dot{m}_{TP,E})_{\theta=n} = \frac{(\dot{m}_{E\to TP,E})_{\theta=n} + (\dot{m}_{TP,E\to ev})_{\theta=n}}{2} \quad (41)$$

$$(\dot{m}_{ev})_{\theta=n} = \frac{(\dot{m}_{TP,E\to ev})_{\theta=n} + (\dot{m}_{ev\to r})_{\theta=n}}{2} \quad (42)$$

$$(\dot{m}_r)_{\theta=n} = \frac{(\dot{m}_{ev\to r})_{\theta=n} + (\dot{m}_{r\to cond})_{\theta=n}}{2} \quad (43)$$

$$(\dot{m}_{cond})_{\theta=n} = \frac{(\dot{m}_{r\to cond})_{\theta=n} + (\dot{m}_{cond\to TP,C})_{\theta=n}}{2} \quad (44)$$

$$(\dot{m}_{TP,C})_{\theta=n} = \frac{(\dot{m}_{cond\to TP,C})_{\theta=n} + (\dot{m}_{TP,C\to C})_{\theta=n}}{2} \quad (45)$$

$$\left(v_{TP,E}\right)_{\theta=n} = \left[\frac{\dot{m}_{TP,E}}{\rho_{TP,E} * a_{TP,E}}\right]_{\theta=n} \quad (46)$$

$$(v_{ev})_{\theta=n} = \left[\frac{\dot{m}_{ev}}{\rho_{ev} * a_{ev}}\right]_{\theta=n} \quad (47)$$

$$(v_r)_{\theta=n} = \left[\frac{\dot{m}_r}{\rho_r * a_r}\right]_{\theta=n} \quad (48)$$

$$(v_{cond})_{\theta=n} = \left[\frac{\dot{m}_{cond}}{\rho_{cond} * a_{cond}}\right]_{\theta=n} \quad (49)$$

$$\left(v_{TP,C}\right)_{\theta=n} = \left[\frac{\dot{m}_{TP,C}}{\rho_{TP,C} * a_{TP,C}}\right]_{\theta=n} \quad (50)$$

$$(Re_{ev})_{\theta=n} = \left[\frac{\rho_{ev} * v_{ev} * d_{ev}}{\mu_{ev}}\right]_{\theta=n} \quad (51)$$

$$(Re_r)_{\theta=n} = \left[\frac{\rho_r * v_r * d_{hyd,r}}{\mu_r}\right]_{\theta=n} \quad (52)$$

$$(Re_{cond})_{\theta=n} = \left[\frac{\rho_{cond} * v_{cond} * d_{cond}}{\mu_{cond}}\right]_{\theta=n} \quad (53)$$

$$(Re_{TP,C})_{\theta=n} = \left[\frac{\rho_{TP,C} * v_{TP,C} * d_{TP,C}}{\mu_{TP,C}}\right]_{\theta=n} \quad (54)$$

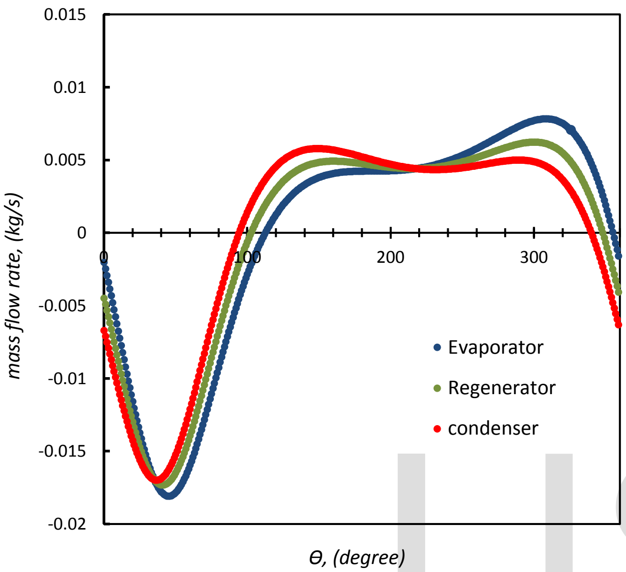

Figure (4) shows the cyclic mass fluctuations through evaporator, condenser, and regenerator.

2.1. Evaporator

The evaporator consists of 265 tubes with an average length of 60 mm and an internal diameter of 2.28 mm. The assembly is a 2-fluid single pass shell and tube heat exchanger. As shown in Fig. 5. (a).

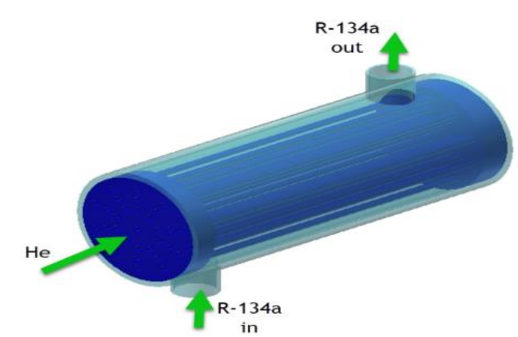

(a)

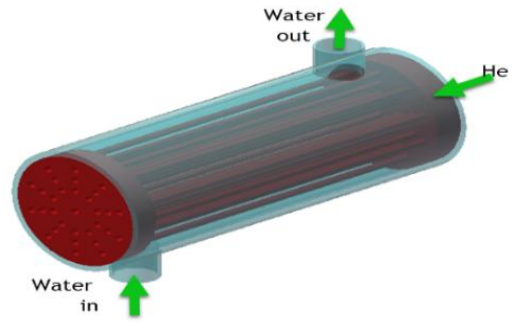

(b)

Figure (5) (a) shell and tube evaporator, (b) shell and tube condenser.

The helium flows inside the tubes of the Shell and tube heat exchanger, the R-134-a flows in the shell side, the R-134-a rate was selected to be constant at 0.1524 Kg/s to get Re=5000. That the cooling energy rate is [23, 24]:

$$\dot{Q_{ev}} = N\int_0^{2\pi} P_E dV_E = UA_{ev,o}(T_{R134-a} - T_E) \quad (55)$$

$$= h_o A_{ev,o}(T_{R134-a} - T_{ev,o})$$

$$= 2\pi k_{ev} L_{ev}(T_{ev,i} - T_{ev,o})$$

$$= h_i A_{ev,i}(T_{ev,i} - T_E) \quad (56)$$

The heat transfer coefficient of the fluid due to its flow through the evaporator is, [25]:

$$Nu = 1.86\,[Re\,Pr\,d/L]^{1/3} \quad (57)$$

$$for\ laminar\ flow$$

$$Nu = 0.023\,(Re)^{0.8}\,(Pr)^{0.4} \quad (58)$$

$$for\ turbulent\ flow$$

The friction factor of the fluid due to its flow through the evaporator is, [26]:

International Journal of Scientific & Engineering Research Volume 10, Issue 2, February-2019
ISSN 2229-5518

$$f = 64/Re \quad (59)$$

$$for\ laminar\ flow$$

$$f = (0.97\, ln\, Re - 1.64)^{-2} \quad (60)$$

$$for\ turbulent\ flow$$

The pressure drops of the fluid due to its flow through the evaporator is, [22, 23]:

$$\Delta p_{ev} = 1.6 \times [f(L/d) \times \rho \times (V^2/2)]_{ev} \quad (61)$$

The values of both h_{ev} and f_{ev} were calculated using the correlations (57), (58), (59) and (60). However, the value of h_{R-134a} was calculated using the following correlation [27]:

$$Nu_{R-134a} = [0.023 Re^{0.8} \times Pr^{0.4}]_{R-134a} \quad (62)$$

2.2. Regenerator

The regenerator has a cylindrical shape, as shown in Fig. 6. It formed of successive circular layers of stainless steel wire net having the same mesh size. The layers are supposed to be homogeneous stacked beside each other without a revolving angle. Mesh of i = 100 pores/in, the length of the regenerator 30 mm and wire diameter of dw = 0.112 mm was proposed for the regenerator fabrication their technical data, [22]. The pressure drop of the gas due to its fluctuation through the regenerator [28]:

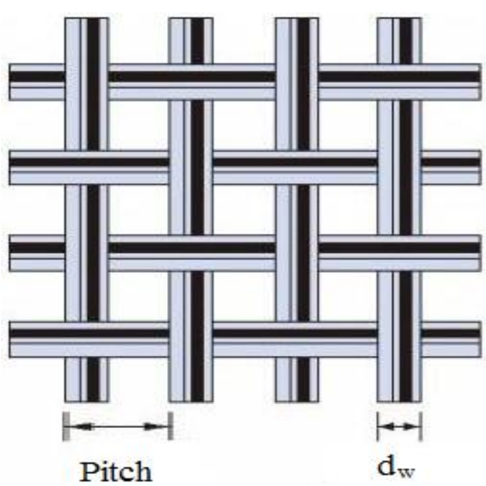

Figure (6) Schematic drawing of wire mesh layer.

$$\log(f_r) = 1.73 - 0.93 \log(Re_r), if\ 0 < Re_r \leq 60 \quad (63)$$

$$\log(f_r) = 0.714 - 0.365 \log(Re_r), if\ 60 < Re_r \leq 1000 \quad (64)$$

$$\log(f_r) = 0.015 - 0.125 \log(Re_r), if\ Re_r > 1000 \quad (65)$$

$$\psi = 1 - \frac{1000i}{25.4} \times \frac{\pi}{4} d_w \quad (66)$$

$$\Delta p_r = f_r \times (L_r/d_{hyd,r}) \times \rho_r \times (v_r^2/2) \quad (67)$$

$$where \quad d_{hyd,r} = \frac{\psi}{1 * \psi} \times d_w \quad (68)$$

The regenerator effectiveness is:

$$\varepsilon = NTU_r/(1 + NTU_r) \quad (69)$$

$$NTU_r = 2 \times \overline{St_r} \times (L_r/d_{hyd,r}) \quad (70)$$

$$St_r = 0.595/(Re_r^{0.4} \times Pr_r) \quad (71)$$

2.3. Condenser

The condenser consists of 285 tubes with an average length of 50 mm and an internal diameter of 2 mm. The assembly is a 2-fluid single pass shell and tube heat exchanger. As shown in Fig. 5. (b). the working fluid is cooled by water during its fluctuation through the compression space. The coolant flow rate was selected to be constant at 0.5058 kg/s to get Re=5000, those that heat rejection rate is [23, 24]:

$$\dot{Q}_{cond} = h_o A_{cond,o}(T_C - T_{cond,i})$$
$$= 2\pi k_{cond} L_{cond}(T_{cond,o} - T_{cond,i})$$
$$= h_i A_{cond,i}(T_{cond,i} - T_{cw}) \quad (73)$$

The heat transfer coefficient of the fluid due to its flow through the condenser is, [25]:

$$Nu = 1.86\,[Re\,Pr\,d/L]^{1/3} \quad (74)$$
$$for\ laminar\ flow$$

$$Nu = 0.023\,(Re)^{0.8}\,(Pr)^{0.3} \quad (75)$$
$$for\ turbulent\ flow$$

The friction factor of the fluid due to its flow through the condenser is, [26]:

$$f = 64/Re \quad (76)$$
$$for\ laminar\ flow$$

$$f = (0.97\,ln\,Re - 1.64)^{-2} \quad (77)$$
$$for\ turbulent\ flow$$

The pressure drop of the fluid due to its flow through the Condenser is, [22, 23]:

$$\Delta p_{cond} = 1.6 \times \left[f\left(\frac{L}{d}\right) \times \rho \times \left(\frac{V^2}{2}\right)\right]_{cond} \quad (78)$$

The values of both h_{cond} and f_{cond} were calculated using the correlations (73), (74), (75) and (76). However, the value of h_{wt} was calculated using the following correlation [27]:

$$Nu_{cw} = [0.023 Re^{0.8} \times Pr^{0.4}]_{cw} \quad (79)$$

The hydraulic losses of the evaporator, regenerator, and condenser were taken into consideration to get the actual pressure inside the expansion and compression spaces that in turn used for calculating cooling energy and coefficient of the performance.

3. Cop Calculation

The elliptic p–V diagrams of the expansion and compression spaces when taking the hydraulic losses into consideration shown in Fig. 7

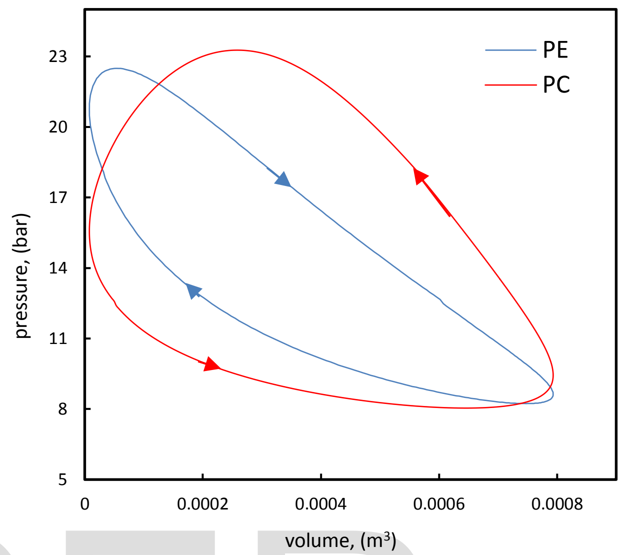

.

Figure (7) P–V diagrams for both expansion and compression spaces.

The designated COP is [14, 23]:

$$\dot{Q_E} = \int_0^{2\pi} P_E\, dV_E \quad (80)$$

$$\dot{Q_C} = \int_0^{2\pi} P_C\, dV_C \quad (81)$$

$$W = -\dot{Q_E} - \dot{Q_C} \quad (82)$$

$$COP = \frac{Q_E}{W} \quad (83)$$

4. Results and Discussion:

A computer program in the form of a spread sheet was arranged to solve the equation numerically, all parameters were calculated instantaneously at the crank angle. The refrigerated space temperature was kept constant at -10 ^0C and the cooling water temperature at 20 ^0C was also kept.

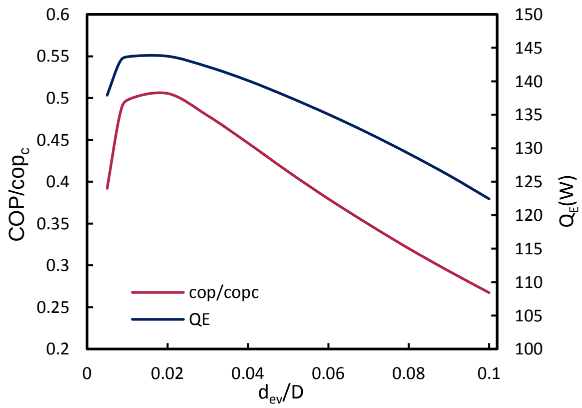

Figure (8) Cooling energy and COP versus inner diameter of the evaporator tube ratio

Referring to figure (8), the increase in evaporator inner diameter decreases Reynolds number and decreases also the convective heat transfer coefficient, but the surface area increases which increase the cooling load. The more increase in the evaporator diameter reduces the cooling load due to the more increase in dead space. The more suitable evaporator inner diameter is about 0.022*D*. Also, the condenser internal diameter is about 0.02*D*, as clear in figure (9).

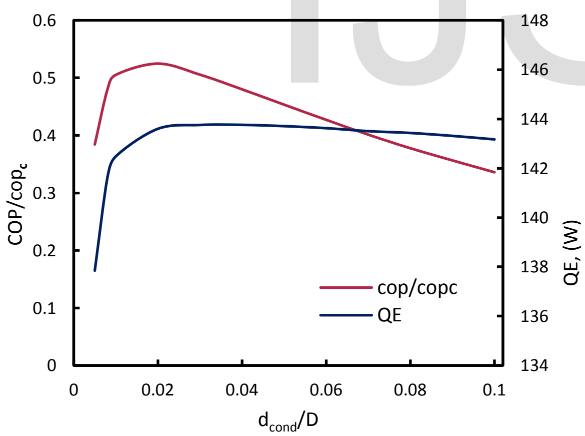

Figure (9) Cooling energy and COP versus inner diameter of the condenser tube ratio.

Referring to figure (10), a sharp reduction in cooling load was observed due to the higher increase in both dead space and pressure losses. The selected evaporator length to get considerable cooling load is 0.6*D*. Also, the selected condenser length to get considerable cooling load is 0.5*D*, as clear in figure (11). The bore was fixed at 0.1 *m*. The diameter of the shell for both evaporator and condenser were fixed to be equal the bore. The dimensions of the heat exchangers, stroke, phase angle, charging pressure, and speed were varied to get the more suitable values that result in higher cooling load and *COP*.

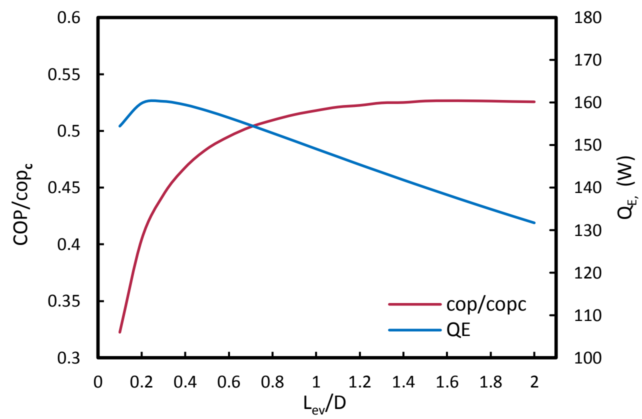

Figure (10) Cooling energy and COP versus length of the evaporator tube ratio

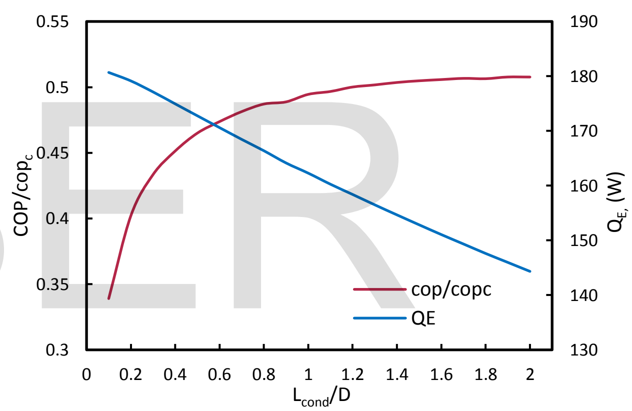

Figure (11) Cooling energy and COP versus length of the condenser tube Ratio.

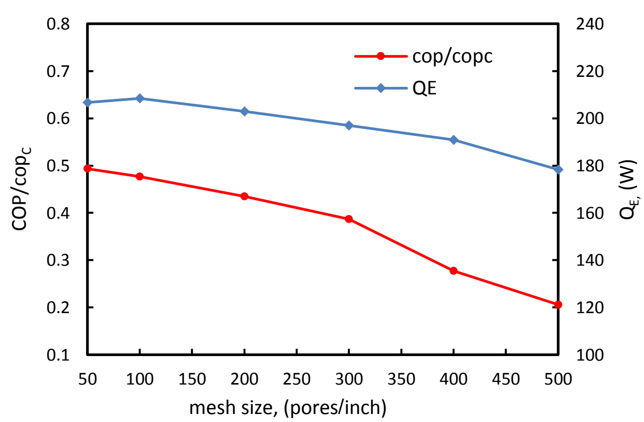

Figure (12) Cooling energy and COP versus the mesh No for SP/D=1 and P_{ch} 1 bar.

Referring to figure (12), the increase in the mesh number reduces the porosity as well as the free flow area which resists the fluctuating of the working fluid, i.e. higher-pressure losses and more required driven power. The more acceptable mesh size is almost 100 pores per inch. Also, the height of the regenerator to called complete effectiveness is about 0.3D as clear from figure (13).

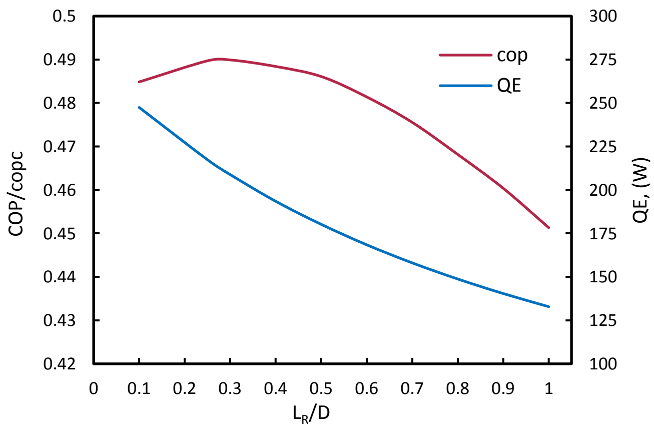

Figure (13) Cooling energy and COP versus the regenerator length for SP1/D=SP2/D=1, mesh 100, and P_{ch}=1 bar

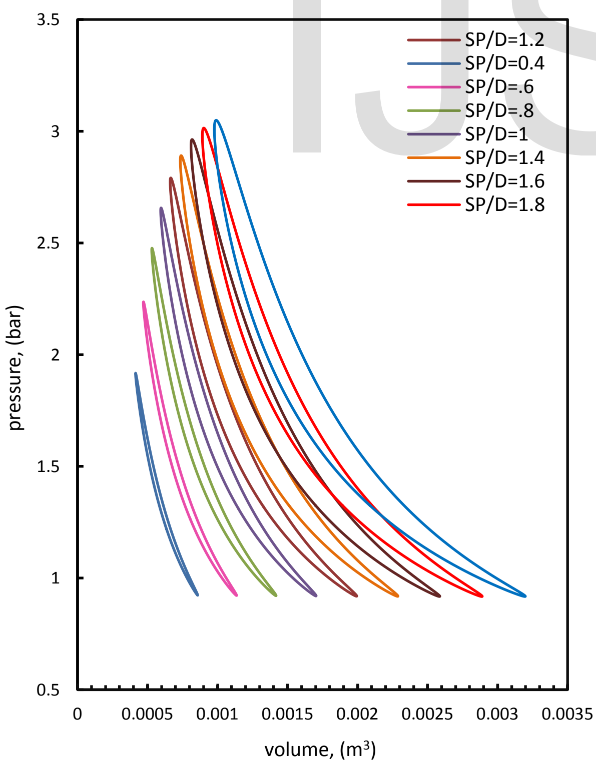

Figure (14) Schmidt p–V diagrams at different piston strokes for mesh 100.

In figure (14), increasing the pistons stroke increases the charged gas which increases the cooling power

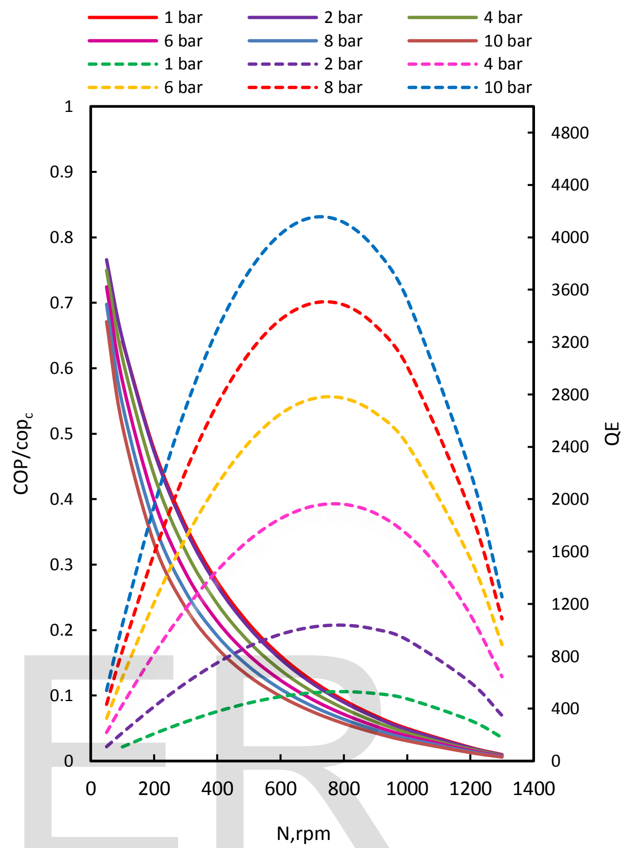

Figure (15) Cooling energy and COP versus N for different charging pressers.

Increase in the piston stroke increases the hydraulic losses, moreover; more increase in hydraulic losses was noted for thin meshes. So, the optimum piston stroke decreases as the mesh size increases. The increasing in the elliptic p–V area due to increase in the piston stroke.

Referring to figure (15), the more charging pressure, and the more cooling load with low *COP*. The refrigerator can develop about 4.0 *kW* if the designer and the manufacturer avoid the leakage problems.

5. Comparison between present work and previous ones

The thermodynamic analysis of a V-type Stirling refrigerator is performed for helium, as the working fluid was investigated by [9]. The V-type integral Stirling refrigerator is achieved for helium, as the working gas was studied by [14]. Figure (16), shows a well-suited and acceptable agreement between present results and previous ones.

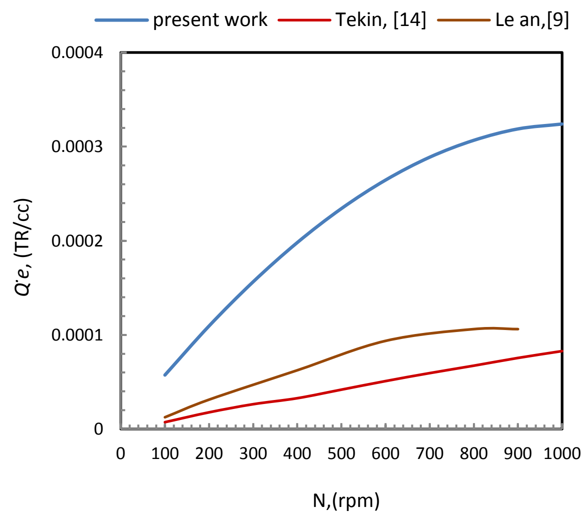

Figure (16) Comparison among present work and previous ones

6. Conclusion

In the present work, the performance of alpha type Stirling refrigerator using shell and tube heat exchanger as an evaporator and a condenser was studied. The main dimensions of the refrigerator that result in higher cooling energy and higher COP were found out in the vision of Schmidt theory. The study monitored the optimum dimensions of the evaporator, regenerator, condenser, piston stroke. The main results can be briefly systemized as the following items:

1. The increase in regenerator length increases the hydraulic losses which decrease the cooling energy. Also, the increase in the regenerator length increases the regenerator effectiveness which increases the COP to reached the maximum at $L_R/D=0.3$ and effectiveness more than 98% and after that, the increase in the regenerator length decreases COP due to the increase of power consumption.
2. The increase in the mesh size decreases the COP and the cooling energy
3. The amount of output cooling energy depends on the pistons strokes, the higher pistons strokes, and the higher cooling energy.
4. The extra charging pressure and speed, the extra cooling energy. The increase in the speed causes a decrease in COP. This is due to the increase in the hydraulic losses which resulted from the increase fluid velocity. The cooling energy increases with increasing the charging pressure. At higher speeds, the cooling energy decreases with increasing the refrigerator speed, the optimum speed is about 750 rpm.

References

1. E. Oguz , F. Ozkadi "Experimental Investigation Of A Stirling Cycle Cooled Domestic Refrigerator", International Refrigeration and Air Conditioning conference, paper.623,(2002).
2. J-F. Sun, et al "Application of Stirling cooler to food processing: Feasibility studyn on butter churning", Journal of Food Engineering, vol. 84, pp. 21–27, (2008).
3. X. Yang, J.N. Chung "Size effects on miniature Stirling cycle cryocoolers", Cryogenics, vol. 45, pp. 537–545, (2005).
4. K. Wang, et al " Stirling cycle engines for recovering low and moderate temperature heat: A review", Renewable and Sustainable Energy Reviews, vol. 62, pp. 89–108, (2016).
5. C. E. Mungan "Coefficient of performance of Stirling refrigerators", European Journal of Physics, vol. 38, pp. 1-9, (2017).
6. A. K. Almajri, et al " Modelling and parametric study of an efficient Alpha type Stirling engine performance based on 3D CFD analysis", Energy Conversion and Management, vol. 145, pp 93–106, (2017).
7. K. Hirata "Schmidt Theory for Stirling Engines", National Maritime Research Institute, pp. 1-9.
8. Kwasi-Effah C. C, et al " Review of Existing Models for Stirling Engine Performance Prediction and the Paradox Phenomenon of the Classical Schmidt Isothermal Model", International Journal of Energy and Sustainable Development, Vol. 1, No. 1, pp. 6-12, (2016).
9. S. Le'an, et al " Performance of a prototype Stirling domestic refrigerator", Applied Thermal Engineering, vol. 29, pp. 210–215, (2009).
10. O. Ercan Ataer, H. Karabulut "Thermodynamic analysis of the V-type Stirling-cycle refrigerator", International Journal of Refrigeration, vol. 28, pp. 183–189, (2005).
11. X.N. He, et al "Design and performance of a room-temperature hybrid magnetic refrigerator combined with Stirling gas refrigeration effect", international journal of refrigeration, pp. 1-7, (2013).

12. P. McFarlane, et al "Experiments with a pressure-driven Stirling refrigerator with flexible chambers", Journal of Applied Physics, vol. 115, pp. 1-7, (2014).
13. T. Otaka, et al "Study of Performance Characteristics of a Small Stirling Refrigerator", Heat Transfer Asian Research, vol. 31, No. 5, pp. 3 44-361, (2002).
14. Y. Tekin, O. E. Ataer "Performance of V-type Stirling-cycle refrigerator for different working fluids", international journal of refrigeration, vol. 33, pp.12–18,(2010).
15. V. V. Trandafilov, M. G. Khmelniuk "Computer simulation of a Stirling Refrigerating machine", Холодильна техніка та технологія,vol. 51, No.5, pp. 92-98, (2015).
16. X.Q. Gao, et al " Design and improvements of a room-temperature magnetic refrigerator combined with Stirling cycle refrigeration effect", International Journal of Refrigeration, v0l.67, pp. 330-335, (2016).
17. H. Hachem, et al "Optimization of an air-filled beta type stirling refrigerator", International Journal of Refrigeration, vol. 76, pp. 296-312, (2017).
18. L. B. Erbay, et al "Overall performance of the duplex Stirling refrigerator", Energy Conversion and Management, vol. 133, pp. 196–203, (2017).
19. V. V. Kishor Kumar , B. T. Kuzhiveli "performance Enhancement of A miniature Stirling Cryocooler with A multi mesh Regenerator design", Journal of Engineering Science and Technology, Vol. 12, No. 6, pp. 1514 – 1524, (2017).
20. H. Ahmed, et al "CFD modelling and parametric study of small scale Alpha type Stirling Cryocooler", Energy y Procedia, vol. 142, pp. 1668-1673, (2017).
21. L.S. Scollo, et al "Twin cylinder alpha stirling engine combined model and prototype redesign", international journal of hydrogen energy, vol. 38, pp. 1988-1996, (2013).
22. E. Eid "Performance of a beta-configuration heat engine having a regenerative displacer", Renewable Energy, vol. 34, pp. 2404–2413, (2009).(18)
23. A.A. El-Ehwany, et al "Development of the performance of an alpha-type heat engine by using elbow-bend transposed-fluids heat exchanger as a heater and a cooler", Energy Conversion and Management, vol. 52, pp. 1010–1019, (2011).
24. Holman JP.Heat transfer. 10^{th} ed. New York: McGraw-Hill Inc; (2010).
25. Cengel, Y.A., 2007. Heat and mass transfer: a practical approach.
26. Li R, Grosu L, Parameter effect analysis for a stirling cryocooler, International Journal of Refrigeration, 80, 92-105, (2017).
27. J. Wen, et al "Experimental investigation on performance comparison for shell-and-tube heat exchangers with different baffles", International Journal of Heat and Mass Transfer, vol. 84, pp. 990–997, (2015).
28. William R Martini "Stirling engine design manual" Washington, (1978).